

# Wave-front sensor strategies for SPHERE: first on-sky results and future improvements

Jean-Francois Sauvage<sup>a,b</sup>, Thierry Fusco<sup>a,b</sup>, Cyril Petit<sup>a</sup>, David Mouillet<sup>c</sup>, Kjetil Dohlen<sup>b</sup>, Anne Costille<sup>b</sup>, Jean-Luc Beuzit<sup>c</sup>, Andrea Baruffolo<sup>d</sup>, Markus E. Kasper<sup>e</sup>, Marcos Suarez Valles<sup>e</sup>, Mark Downing<sup>c</sup>, Philippe Feautrier<sup>c</sup>, Laurent Mugnier<sup>a</sup>, Pierre Baudoz<sup>f</sup>,  
<sup>a</sup> **Onera - The French Aerospace Lab, BP 72, 92322 Châtillon, France**

<sup>b</sup>Laboratoire d'Astrophysique de Marseille

<sup>c</sup>Institut de Planétologie et d'Astrophysique de Grenoble

<sup>d</sup>Osservatorio Astronomico di Padova

<sup>e</sup>European Southern Observatory

<sup>f</sup>Laboratoire d'Etudes Spatiales

**Jean-francois.sauvage@onera.fr**

## ABSTRACT

SPHERE instrument [1] (Spectro-Polarimetry High-contrast Exoplanet Research) is a second generation ESO instrument dedicated to high contrast imaging, and exoplanet direct detection and characterisation. The overall performance of XAO system of SPHERE, as well as the optimal control law for turbulence correction, are presented in dedicated papers [5,6]. The global performance of the instrument and of all observing modes of SPHERE is done in [4].

The strategy of Wave-front Sensing [WFS] in SPHERE relies on two faces, and is thoroughly discussed in this paper.

Firstly, extreme adaptive optics (XAO) is required for both turbulence and quasi-static pattern compensation. Particularly, the high frame rate and large subaperture numbers of the Shack-Hartmann WFS allows SAXO to optimally measure and compensate for atmospheric turbulence. Moreover, the spatial filtering [7,8] allows one to deepen the contrast curve, and is automatically adjusted on turbulence level to provide the best performance. Finally, a dedicated calibration procedure based on focal-plane wave-front sensing is optimized for NCPA compensation on the coronagraphic device, ensuring the best compensation of quasi-static speckle. Secondly, a high robustness to faint magnitude guide star allows SAXO to address a large panel of targets for exoplanet detection and characterization. This is only made possible by the joint use of a dedicated Wave-Front Sensing for turbulence, EMCCD detector capability, and adaptation of the system to the star magnitude. The noise propagation has been carefully monitored and optimized. The weighted center of gravity gives an optimal trade-off between performance with respect to noise, and complexity of implementation. The use of an EMCCD detector allows a powerful noise reduction on the wave-front sensor detector. And finally, 5 SAXO observing modes are defined in order to cover all star magnitudes up to 16, with systematic optimal performance. During the whole assembly integrations and test period, choices have been done to optimise the trade-off between performance, robustness, and simplicity of use. The self-adaptation and auto-calibration of the instrument has been a strong investment, as well as developing a great simplicity of use. We describe here the actions taken to reach this level of operation for SPHERE. Finally, perspective are withdrawn for improving the strategy of WFS in the framework of future XAO instrumentations in E-ELT.

**Keywords:** Extreme Adaptive Optics, wave-front sensing, focal-plane wave-front sensing

## 1. INTRODUCTION

The search for exoplanets is surely one of the most attractive goals of today's astronomy, as it tends to give a first attempt of answer to the question of life out of earth. The direct imaging of exoplanets is particularly helpful in the characterization of exoplanets, as the photons coming from the exoplanet are the witness of the components of its atmosphere, and may therefore reveal the presence of methane or oxygen in it. But the direct imaging is also one of the most challenging goals for instrumental science, as the photons coming from the exoplanet are hidden in a million more coming from the host star, and strongly disturbed by both the atmospheric turbulence and the observing instrument itself.

The SPHERE instrument is a second-generation high contrast multi-imaging instrument, developed under IPAG responsibility since 2004, integrated at Grenoble during the last two years, and currently under commissioning period at VLT observatory. In order to deal with the severe observation conditions described below, this instrument combines an eXtreme Adaptive Optics [XAO] correction stage, able to compensate optimally for the fast-evolving atmospheric turbulence, three additional loops able to deal with the slow-evolving pupil position, PSF centering on coronagraph, and Non-Common-Path Aberrations static patterns. Moreover, the system includes different choices of coronagraphic stages able to physically cancel the majority of the stellar flux, and smart and dedicated post-processing methods drawing the pith and marrow of the instrument performance.

## 2. FIRST LIGHT FOR EXTREME AO SYSTEM OF SPHERE

The different correction loops of SAXO are detailed here:

First of all, the main SAXO loop (called VIS loop) is designed to compensate for the short time-scale (millisecond) turbulent variation of the optical aberrations.

Strategy of WFS for SPHERE is two-fold:

- **eXtreme Adaptive Optics (XAO)** for both turbulence and quasi-static pattern compensation.
  - High frame rate

This loop has to be extremely fast (original frequency 1200Hz, finally working at 1380Hz), and presents a two-stages correction device (Tip-Tilt mirror ITTM, and High Order Deformable Mirror HODM) both working at 1200Hz.

- Large subaperture numbers of Shack-Hartmann

The size of the corrected area in the focal plane directly depends on the number of subapertures of the Shack-Hartmann, and the number of actuators of the deformable mirror. In order to reach a area diameter of 1.6 arcsec in H band, the number of subaperture has been chosen to 40x40, and the number of actuators (in Fried geometry) has been set to 41x41.

- Spatial filtering

The Hartmann-Shack wave-front sensor is known to be strongly sensitive to the high spatial frequencies of the phase (higher than 20 cycles / pup), and therefore introduces a strong aliasing in the measurement. In order to release this limitation, a spatial filter installed in the focal plane at the entrance of WFS path is installed in order to physically remove the high spatial frequencies. Its size has to be adapted to the turbulence conditions in order to give its optimal behavior.

- Focal-plane wave-front sensing for NCPA compensation

The final performance of a high contrast imaging system is known to be due to the residual static aberration unseen and therefore uncorrected by the loop (called Non Common Path Aberrations NCPA). In order to compensate for them, the system uses a dedicated focal-plane wave-front sensor called “phase diversity”.

- High robustness to **faint magnitude** guide star to address a large panel of targets
  - Dedicated Wave-Front Sensing for turbulence, EMCCD detector capability,
  - Adaptation of the system to the star magnitude.

In order to cover all flux / seeing conditions, **only 6 AO modes** are defined. These modes will use different parameters / device to increase the handle the flux range corresponding to a guide star magnitude from 1 to 14. These parameters are:

- Gain of the EMCCD VisWFS detector. This gain varies from 1 to 1000.
- Spectral filter width, using red (780-900nm) filter improves WFS quality, but using blue filter (475-900nm) increases the flux on detector
- Last, the frequency of the detector allow to increase the exposure time. Three frequencies are considered, 1200 (nominal), 600 and 300Hz.

The Figure 2 shows the characterisation of the PSF shape and quality (Strehl Ratios @ 1.6µm are given) for different R magnitude from 8.6 to 15.4. The turbulence, generated optically by a turbulence simulator, are chosen representative of Paranal conditions (12m/s, 0.85arcsec seeing). The corresponding Strehl Ratii obtained in lab confirm that the instrument fulfills the specifications (90%SR obtained at magnitude 9) and covers more than reasonably the magnitude range expected.

The on-sky performance obtained during first period of commisionning (10 to 21 of may, 2014) are gathered on

Figure 3. The performance (Strehl Ratio) is plotted with respect to flux. Of course, the conditions of turbulence are not controled as in laboratory, and the result of this plot gather seeing ranging from 0.4 to 1.7 arcsec. This is to be taken into account in the interpretation of this plot. The global bevhaviour of the performance with respect to flux fully agrees with the numerical simulations, and the laboratory results : the performance is constant for bright magnitude (up to magnitude 10), and decreases for fainter magnitude, reaching an impressive Strehl Ratio of 30% at magnitude 13 (faintest star tested during COM1). For magnitude brighter than 10, the value of the plateau in Strehl is around 72% Strehl Ratio. This value is expected to be 15 to 20% higher, revealing a limitation still under investigation. The actual interpretation is to make a link between this loss and with a strong residual jitter (10 mas instead of 3 mas, which could fully explains the 15% loss in term of Strehl Ratio).

|  | SAXO Visible CONFIGURATION |         |         |         |         |         |
|--|----------------------------|---------|---------|---------|---------|---------|
|  | 1000                       | 1000    | 1000    | 1000    | 30      | 1       |
| CCD Gain   | 1000                       | 1000    | 1000    | 1000    | 30      | 1       |
| WFS spectral filter                                    | F0                         | F0      | F0      | F4      | F4      | F4      |
| Loop frequency [Hz]                                    | 300                        | 600     | 1200    | 1200    | 1200    | 1200    |
| Peak flux in one subaperture [ADU]                     | 1,5E+04                    | 1,5E+04 | 1,5E+04 | 1,5E+04 | 1,5E+04 | 1,5E+04 |
| Source flux at detector level [electron/seconds/pupil] | 6,2E+08                    | 1,2E+09 | 2,5E+09 | 7,5E+09 | 2,5E+11 | 2,8E+13 |
| Rmag corresponding to Peak flux L37 : saturating VWFS  | 7,3                        | 6,5     | 5,8     | 4,6     | 0,8     | -4,4    |
| Peak flux in one subaperture [ADU]                     | 1,0E+02                    | 1,0E+02 | 1,0E+02 | 1,0E+02 | 1,0E+02 | 1,0E+02 |
| Source flux at detector level [electron/seconds/pupil] | 1,6E+07                    | 3,1E+07 | 6,2E+07 | 1,9E+08 | 6,3E+09 | 1,9E+11 |
| Rmag corresponding to Lower flux                       | 11,3                       | 10,5    | 9,8     | 8,6     | 4,7     | 1,1     |

Figure 1: Detail of the 6 AO modes defined for SPHERE XAO system. The framerate and the spectral filter are adapted in order to cover the full range of magnitude to be addressed b y SPHERE.

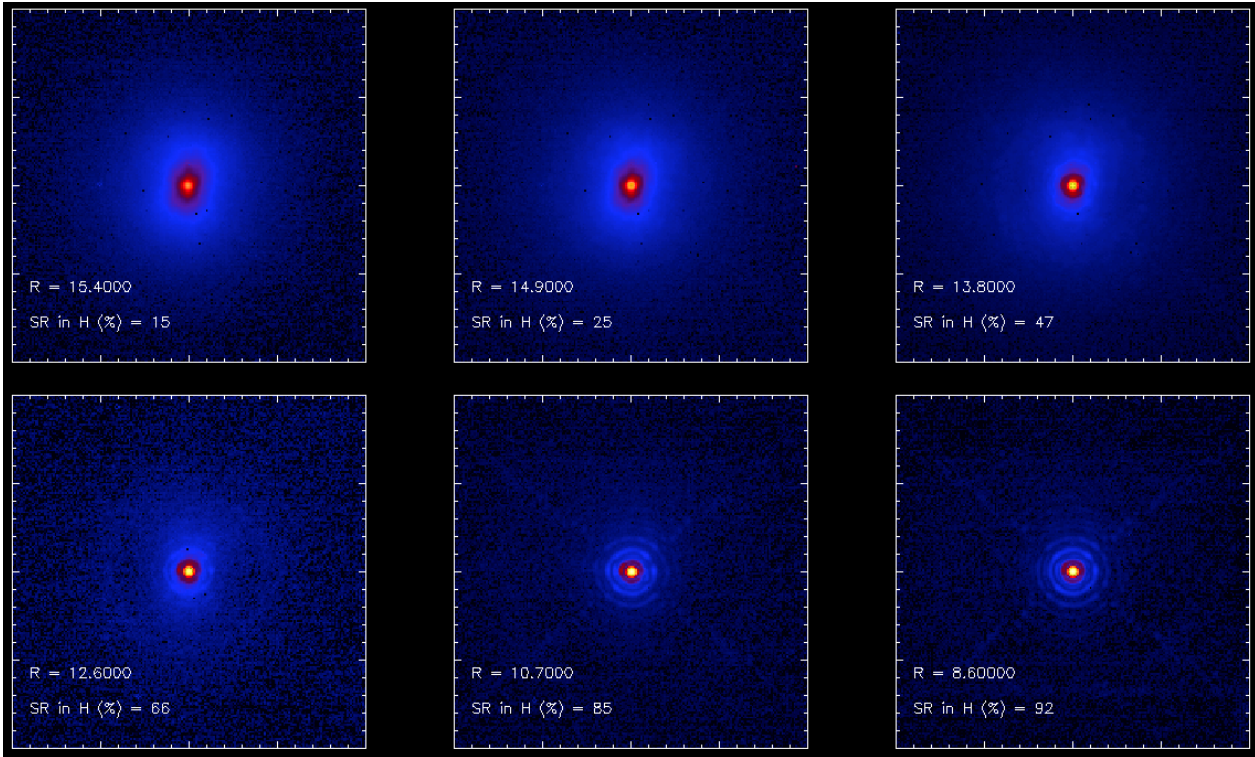


Figure 2: various PSF shape for SPHERE, obtained in lab during AIT at Grenoble, for various conditions of guide star R magnitude. Wind speed is nominal at 12m/s.

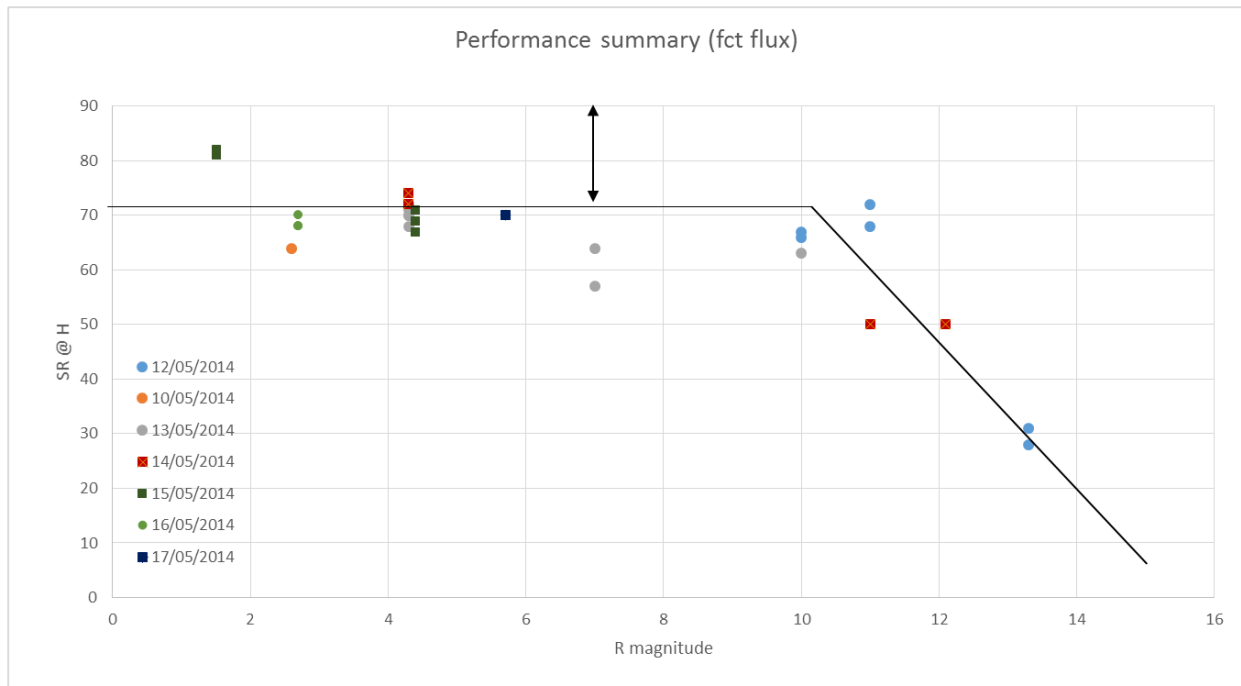


Figure 3: on-sky performance of SPHERE XAO system. Strehl ratio @ 1.6 microns, given with respect to guide star R magnitude.

### 3. IMPROVED WAVE-FRONT SENSING:

#### 3.1 Spatially filtered shack-hartmann

SAXO WFS is based on a spatially-filtered Shack-Hartmann WFS. The role of the spatial filter is to remove (or decrease) the aliasing effect in wave-front sensing ([7]). The aliasing effect is one of the main limitations of the extreme extinction. Without correction, this effect of high frequency folding on the WFS measurement will create diffuse light residuals inside the corrected area, due to the uncorrected high frequency. The spatial filter consists in placing a pinhole in the focal plane upstream of the WFS camera. This pinhole allows to remove physically the light far from the optical axis (hence to suppress the high spatial frequencies of the aberrated wave-front) and therefore to limit the aliasing effect.

The spatial filtering has been validated in laboratory, showing regular behaviour with high frequency. The only problem is that in lab, it has been impossible to close the spatial filter to the theoretical size foreseen ( $1.1 \lambda/d$ ,  $d$  being the subaperture size). This problem is due to the high spatial frequencies residuals of the turbulence simulator used during integration, coupled to the high spatial frequencies of High Order Deformable Mirror, that did not allow to close Spatial filter smaller than  $1.3 \lambda/d$ . On-sky, the spatial filter has shown impressive results. Figure 4 shows coronagraphic images of star HD140573, for various sizes of spatial filter, from  $1.9 \lambda/d$  down to  $1.1 \lambda/d$ . The impact of aliasing reduction is clearly visible on the whole corrected area, where the diffuse light coming from aliasing effect is impressively reduced when closing the filter.

The spatial filter impact has been demonstrated in two different conditions of turbulence, faint (Figure 5 [left]) and nominal (Figure 5 [right]). The coronagraphic profiles (azimuthal average of flux wrt separation to the star) shows the expected impact of spatial filter, deeping the contrast on all the focal plane especially close to the AO cut-off. Apart from the performance of spatial filter, the selection of the size of spatial filter is made automatically with respect to turbulence strength.

The Figure 6 shows comparison of the experimental coronagraphic profiles (on-sky data) with the end-to-end simulation result for faint turbulence condition at  $1.1 \lambda/d$ . The very good match between simulation and on-sky data is impressive and fully validates the system behaviour.

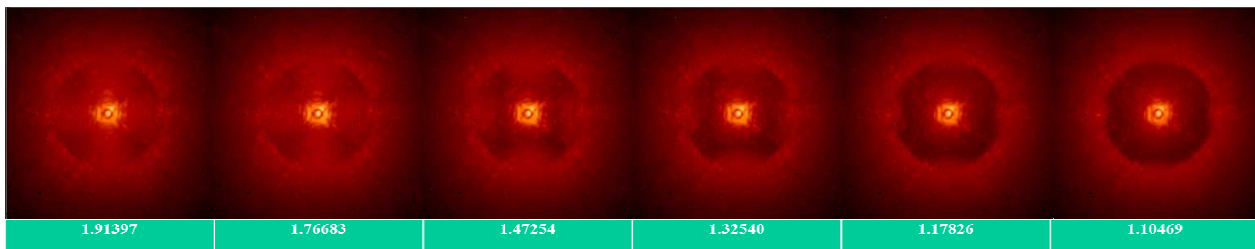
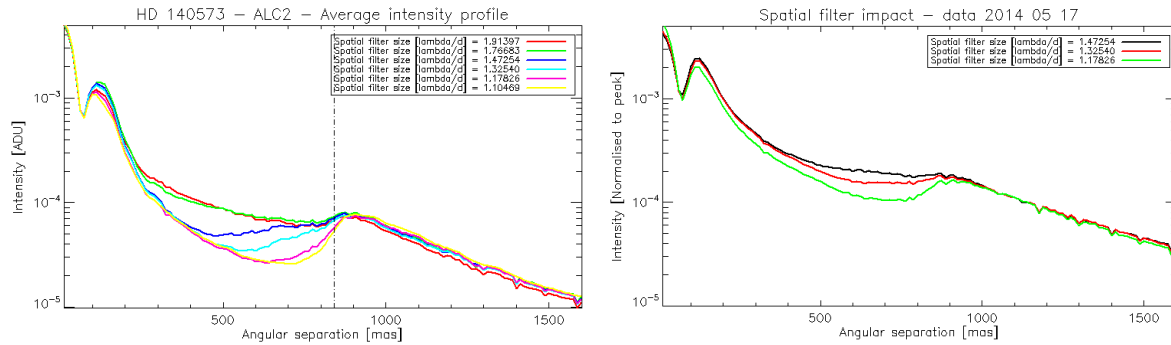
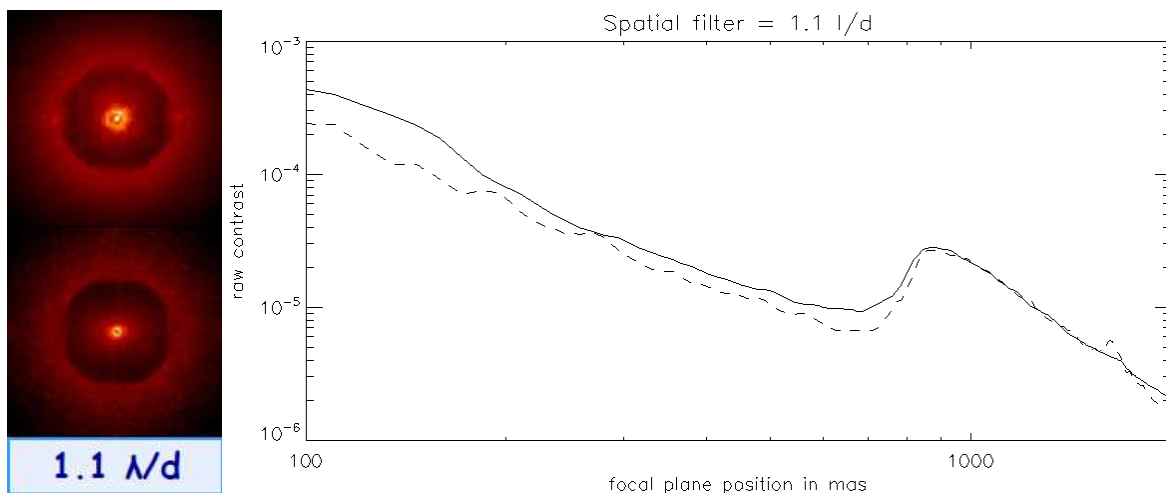


Figure 4: Coronagraphic image (combination apodised Lyot coronagraphic) of star HD140573, for various sizes of spatial filter, from  $1.9 \lambda/d$  down to  $1.1 \lambda/d$ . Imaging wavelength is H2 (1.6 microns).



**Figure 5: Impact of spatial filtering. [Left] azimuthal profiles of coronagraphic image of HD140573, for faint turbulence conditions. [right] azimuthal profiles of coronagraphic image of star alpha Regulus HR 3982, for nominal turbulence conditions.**



**Figure 6: impact of spatial filter at small sizes (and faint turbulence conditions), and comparison to end-to-end simulation.**

### 3.2 High temporal stability

The temporal stability of “quasi”-static speckles residuals is a key point for reaching the final SAXO performance and SPHERE detection capacity.

PSF stability has been demonstrated on sky with SPHERE, one example is done by performing long exposure non-coronagraphic images on bright star and watch for speckles temporal evolution. The Figure 7 shows such a result, with saturated PSF, at two moments separated from 20 minutes. The PSF speckle show great similarities in shape and therefore enhances the whole instrument stability.

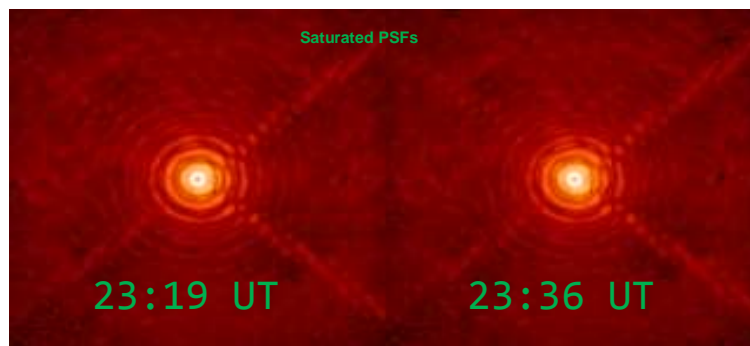


**Figure 7: Estimated SR = 83 % (on un-saturated PSF) – seeing  $\sim 0.7$ , saturated non-corono images, separated by 20 minutes.**

## 4. COMPENSATION OF STATIC RESIDUAL : NCPA STUDY

### 4.1 Baseline solution: classical phase diversity

The last limitation to high contrast lies in the Non-Common Path Aberrations. These optical static aberrations are situated on the imaging path, and are therefore not seen and not corrected by the AO system. In order to reach the final performance of the system, the solution designed for SPHERE consists in a focal-plane estimation of these aberrations, and a compensation by the AO system itself. The focal-plane estimator chosen for estimating these aberration is the technic of Phase Diversity [7], able to retrieve aberrations from a set of two focal-plane images (One in-focus, and one out-of-focus). The compensation is done by modifying the reference slopes of the WFS accordingly, so as the closed-loop naturally compensates from the measured aberrations.

### 4.2 During AIT: validation of the principle

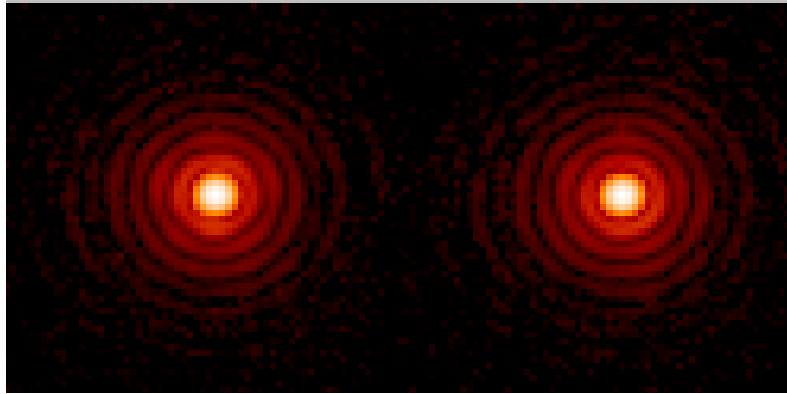
The method is validated on SPHERE during AIT at Grenoble, and allows to reach very high Strehl Ratio on internal source. The Figure 8 shows the internal PSF of SPHERE. On left side, NCPA non-compensated. On right side, NCPA compensated by the baseline solution. The Strehl Ratio increases from 97.5 to 99.0 % in H band, reducing the residual NCPA from 41 down to 25nm RMS. It is to be noted that the first performance of 97.5% in H already fulfills the specifications, which are 43nm RMS of residual on all frequencies.

Later on the integration, some limitations are identified to the method:

- The **increasing number of dead actuators** of the deformable mirror HODM (CILAS), from 2 (initial number) to 17 (actual number) impacts the performance. The dead actuators present a high spatial frequency pattern in the phase in pupil plane, that are difficult to estimate with the implemented version of phase diversity algorithm.
- The **dependency of HODM shape to temperature** introduces two effects:
  - Even if the low order aberrations of HODM (focus and astigmatism) are corrected by the dedicated active Toric Mirror 3, the variation of the high spatial frequencies amplitude strongly impacts the NCPA estimation.
  - The evolution of the global shape of HODM, even if corrected by TM3, makes the residual pattern due to dead actuators also evolves with temperature.
- **Pupil transmission** (including Gaussian illumination shape), even rather flat, impacts a lot on phase diversity estimation. The internal calibration lamp used to perform the measurement presents a pupil transmission varying with time, and therefore requires to be calibrated before the NCPA estimation itself.
- **Differential centering** between focus / defocus images is introducing a bias in the measurement.

The conclusion of this study after reintegration at the telescope is:

- HODM shape is favorable **at lower temperature**
- The ultimate performance (overall optical internal quality and alignment) is estimated at **(97.2SR@H2 – 42nmRMS)** at 12°C (average temperature at UT3 dome) and is already in spec: very small improvements made by current implemented method.
- Optimised phase diversity algorithm should be able to further improve the performance.



|            | Ref slope : WFS path only | REFSLP+ NCPA           |
|------------|---------------------------|------------------------|
| S<br>R @ H | $97.5 \pm 1\%$            | $99.0 \pm 1\%$         |
| R<br>MS    | $41 \pm 10 \text{ nm}$    | $25 \pm 10 \text{ nm}$ |

Figure 8: internal quality of SPHERE system, before and after NCPA compensation.

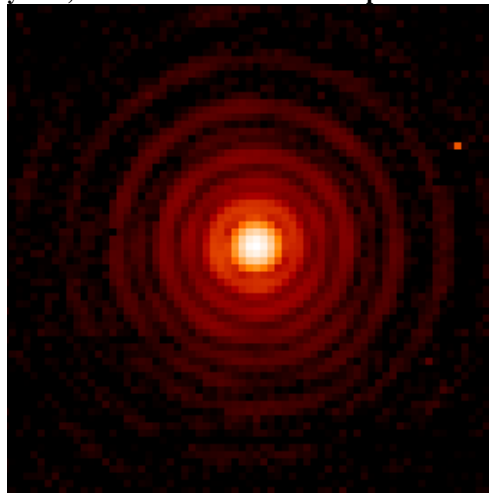


Figure 9: Internal quality of instrument, as installed on telescope is estimated at 97.2% in H2 band (42nm RMS residual).

#### 4.3 Toward improved estimation

The whole operation at commissioning 1 is performed with no NCPA compensation. Meanwhile, the phase diversity algorithm is improved to account for new features:

- Take into account the **pupil transmission map and illumination**. This map can be easily calibrated by the system (IRDIS pupil imaging mode) and used during phase diversity estimation (see Figure 10).
- Account for **differential centering** between focus and defocus images, this will become a new parameter estimated by phase diversity
- **Demonstrate** the optimised phase diversity algorithm on tricky phase map estimation, and allow a further modification of the phase diversity algorithm.

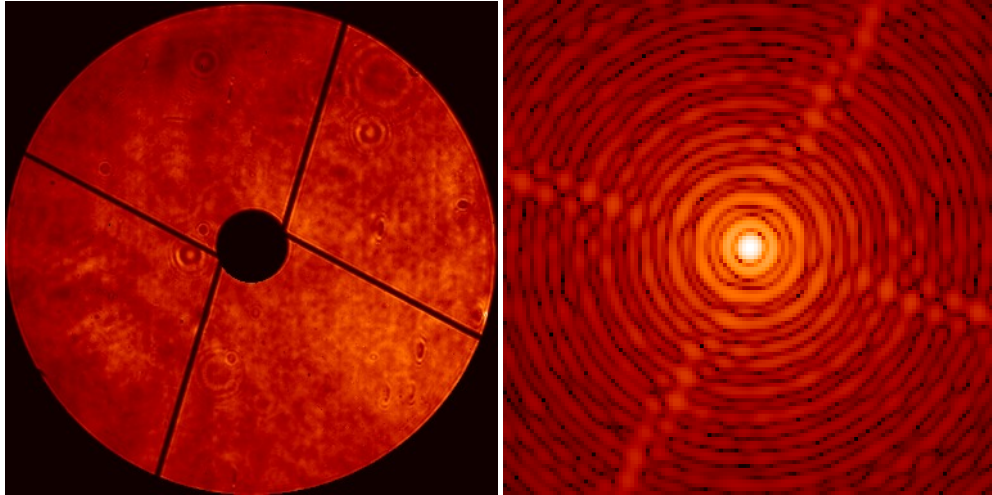


Figure 10: pupil image of SPHERE, seen in the IR (H2 band), and simulated PSF with amplitude-only effects. SR of 99.7% is estimated on the right simulated PSF.

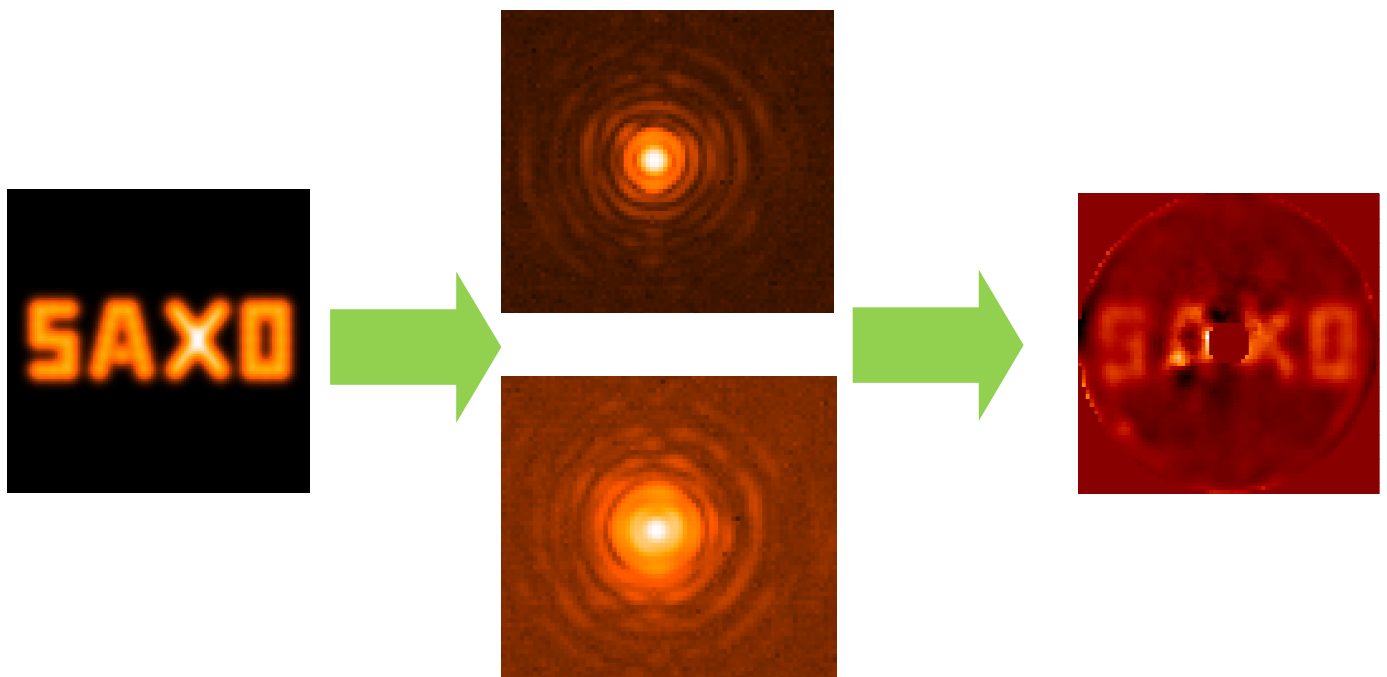


Figure 11: Experimental validation of optimized NCPA algorithm on SPHERE instrument.  
 [left] introduction of a given pupil phase aberration containing high spatial frequencies.  
 [center] experimental set of two focal-plane images (H2) [top : focused] [bottom] = out of focus.  
 [right] phase map aberrations estimated by optimized phase diversity. The high spatial pattern SAXO is clearly visible and correctly estimated.

## 5. CONCLUSION

The wave-front sensor strategy of SAXO, the eXtreme Adaptive Optics of SPHERE, has been extensively demonstrated in lab and on-sky. In this paper, some detailed analysis of on-sky results have been highlighted and validated.

The performance with flux shows the nominal behavior, with a high and constant performance up to magnitude 10, and the highest R magnitude of 13 demonstrated on sky (no fainter star has been observed up to now). 6 AO modes defined to deal with large magnitude range of guide star. Spatial filtering impact has been demonstrated, and shows a great improvement of the contrast. These points (AO modes, spatial filter sizes) are chosen automatically by the system during operation.

The NCPA on SPHERE are small enough to avoid using the baseline originally designed for the instrument. Demonstration has been made that a higher quality can be reached by using an optimized algorithm.

The wave-front sensor strategy of SAXO, initially designed in 2004 [2], delivers now its full capacity on-sky and demonstrates the full performance of the instrument, promising some fruitful astronomical results for the coming years.

This work was partly funded by the European Commission under FP7 Grant Agreement No. 312430 Optical Infrared Coordination Network for Astronomy and by the Office National d'Etudes et de Recherches Aérospatiales (ONERA) (in the framework of the NAIADÉ Research Project).

## REFERENCES

- [1] J.-L. Beuzit, D. Mouillet, C. Moutou, K. Dohlen, P. Puget, T. Fusco, and A. Boccaletti, "A planet finder instrument for the VLT," in *Proceedings of IAU Colloquium 200, Direct Imaging of Exoplanets: Science & Techniques* (Cambridge University Press, 2005), pp. 317–323
- [2] T. Fusco *et al* "High-order adaptive optics requirements for direct detection of extrasolar planets: Application to the SPHERE instrument" *Optics Express*, Vol. 14, Issue 17, pp. 7515-7534 (2006)
- [3] J-F Sauvage J.-F., Fusco T., Rousset G., Petit C., "Calibration and Pre-Compensation of Non-Common Path Aberrations for eXtreme Adaptive Optics", *JOSA A*, Vol. 24, Issue 8, pp. 2334-2346 (2007)
- [4] J.-L. Beuzit *et al*, "SPHERE: a planet finder instrument for the VLT", paper 9148-17, this proceeding
- [5] T. Fusco *et al* "Final performance and lesson-learned of SAXO, the VLT-SPHERE extreme AO From early design to on-sky results", paper 9148-63, this proceeding
- [6] C. Petit *et al* "SPHERE eXtreme AO control scheme: final performance assessment and on sky validation of the first auto-tuned LQG based operational system", Paper 9148-23, this proceeding
- [7] L.A.Poyneer and B. Macintosh, "Spatially filtered wave-front sensor for high-order adaptive optics", *JOSA A*, Vol. 21, Issue 5, pp. 810-819 (2004)
- [8] T. Fusco *et al* "Closed-loop experimental validation of the spatially filtered Shack-Hartmann concept", *Optics Letters*, Vol. 30, Issue 11, pp. 1255-1257 (2005)